

DIURNAL PROPAGATING PRECIPITATING SYSTEMS TO THE NORTH OF NEW GUINEA ISLAND: IN-SITU OBSERVATION OF INTERNAL STRUCTURE AND AMBIENT ATMOSPHERE

Masaki KATSUMATA*, Kunio YONEYAMA and Hisayuki KUBOTA
*Institute of Observational Research for Global Change,
 Japan Agency for Marine-Earth Science and Technology
 (JAMSTEC/IORGC), Yokosuka, Japan*

1. INTRODUCTION

The tropical western Pacific is characterized by high SST and large amount of precipitation. The accumulated warm water in the region, so-called "warm pool", is one of the important factors of El Nino.

Among the factors affecting the warm pool, precipitation is the important one as, for example, fresh water flux to make "the barrier layer" (Lukas and Lindstrom, 1991). The precipitating systems also affected to the ocean by the wind stress which drive the surface water, especially as the trigger of El Nino by the "westerly burst" accompanying MJO convectively active phase.

The one of the significant and important characteristics of the precipitation in the tropics is the diurnal cycle, even over the ocean (Nitta and Sekine, 1994). Chen and Houze (1997) pointed that the diurnal cycle is an important element in the MJO.

While many studies explain the mechanism as the vertical one-dimensional processes, some studies revealed the diurnal precipitating features propagated from the land to the ocean and affected diurnal cycle of the oceanic precipitation (e.g. Houze et al., 1981; Yang and Slingo, 2001; Mapes et al, 2003; Mori et al., 2004). In the tropical western Pacific, Liberti et al. (2001) revealed that the precipitation over the warm pool is also affected by the land effect of New Guinea Island and other small islands. However, their results were based on the satellite infrared images, which sometimes cannot reflect the behavior of the precipitating systems below the cloud top.

In the past four years, we JAMSTEC have been carried out the observation of the equatorial precipitating systems and the ambient atmosphere over the warm pool by deploying our research vessel (R/V) *Mirai* at (2N, 138E) stationary for weeks to a month in the every boreal autumn or winter. In the present study, we investigated the diurnal cycle of the precipitating systems over the warm pool by using the data from the shipborne Doppler radar, which can detect the behavior of the precipitating systems

directly. The map around the observation point is shown in Fig. 1.

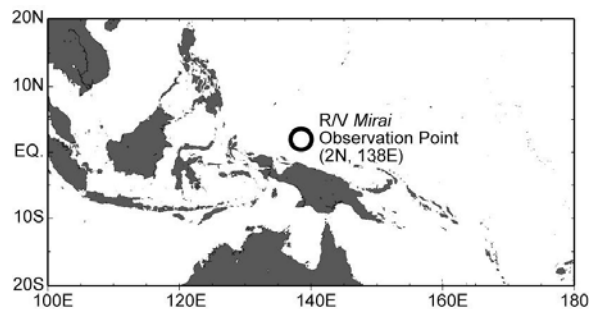


Fig. 1: The map around the R/V *Mirai* observation point (2N, 138E)

2. OBSERVATION PERIODS

The stationary observations of R/V *Mirai* at (2N, 138E) have been carried out in every boreal autumn or winter from 2000/2001 to 2003/2004, as shown in Table 1. The convectively active periods of MJO are within the observation period in MR00-K07, MR01-K05 and MR04-01. The convectively inactive periods are in MR00-K07, MR01-K05 and MR02-K06. The local time of the point is 9 hours ahead of UTC (LST = UTC + 9h).

Year Code	Start End	Days	Characteristics
2000 MR00-K07	Nov.28 Dec.10	13	Incl. latter half of MJO active period
2001 MR01-K05	Nov.09 Dec.09	31	Incl. beginning of MJO active period
2002 MR02-K06	Nov.22 Dec.12	21	All inactive, but MJO signal passed over
2004 MR04-01	Mar.02 Mar.15	13	Incl. beginning of MJO active period

Table 1: The periods of the observations used in this study.

3. OBSERVATION INSTRUMENTS AND DESIGN

The principle meteorological instruments on R/V *Mirai* are the C-band (5-cm in wavelength) Doppler radar and radiosonde launcher. The continuous observation of the C-band Doppler radar was carried

* Corresponding author address: Masaki KATSUMATA, Institute of Observational Research for Global Change, Japan Agency for Marine-Earth Science and Technology (JAMSTEC/IORGC), Natsushima-cho 2-15, Yokosuka 237-0061 JAPAN; e-mail: katsu@jamstec.go.jp

out for every cruise, by repeating a cycle every 10 minutes. One cycle consisted of (1) surveillance PPI (at the elevation of 0.5 degree, for 200-km in range distance, to obtain reflectivity), (2) volume scan (at 21 elevations, for 120-km in range distance, to obtain reflectivity and Doppler velocity), and (3) optional RHIs (for 120-km in range distance to obtain reflectivity and Doppler velocity). The noise filtering in the post processing is as in Katsumata et al (2005).

The radiosonde observations were also carried out every 3 hours through each observation period. The pre-launch calibration procedures were after Yoneyama et al. (2002).

4. GENERAL DIURNAL CHARACTERISTICS OF PRECIPITATION

To extract the general diurnal characteristics of the precipitation, first we used the radar echo area with the reflectivity stronger than 15 dBZ at every 1 hour. The diurnal tendency is presented by calculating ratio of the echo area in the snapshot to the running mean for 25 hours, i.e.

$$R(h_0) = A(h_0) / \left(\sum_{h=h_0-12}^{h_0+12} A(h) / 25 \right) \quad (1)$$

where h_0 is the target time, $R(h_0)$ is the ratio to obtain, $A(h)$ is the radar echo area at the time h .

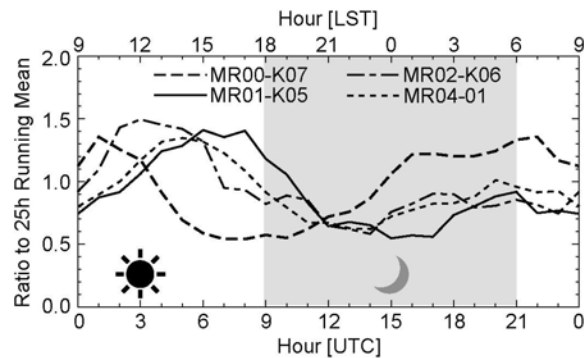


Fig. 2: Diurnal variation of the radar echo area (> 15 dBZ), represented by averaging the ratio to 25-hour running mean for each hour ($R(h_0)$ in Eq.(1)).

Figure 2 is the plot of averaged $R(h_0)$ for each hour and each observation period. The figure shows that the lines have two peaks within a day, at around local afternoon (12-18LT) and local midnight to dawn (0-6LT). Among the peaks, the former is larger in MR01-K05 (including convectively active period), MR04-01 (active period) and MR02-K06 (inactive period), while latter in MR00-K07 (including both active and inactive period). The former peak corresponds to that in Liberti (2001). The northward propagation from New Guinea island to the north, including the observation point (2N, 138E), is also observed in GMS (or GOES) infrared (IR) images.

5. DIURNAL APPEARING MESOSCALE CONVECTIVE SYSTEMS

The all of observed MCSs are categorized from their morphological characteristics into four: (1) with arc-shaped leading edge of about 100km horizontal scale, (2) with straight linear- or band-shaped leading edge but not reached (2N, 138E), (3) with straight linear- or band-shaped leading edge and passed over (2N, 138E), and (4) northward propagating precipitating area without significant leading edge. (The example of radar PPIs for types (2), (3) and (4) are shown in Fig. 3.) The latter three types, types (2), (3) and (4), frequently appeared in local afternoon, i.e. diurnal peak of the echo area, while type (1) appeared non-diurnally.

Among the diurnal MCSs, type (2) has straight linear-shaped convective leading edge and trailing stratiform region, while type (4) consists of widespread echo area and no significant convective leading edge. The type (3) is the hybrid type of them, i.e. the band-shaped with the width of several tens of kilometers.

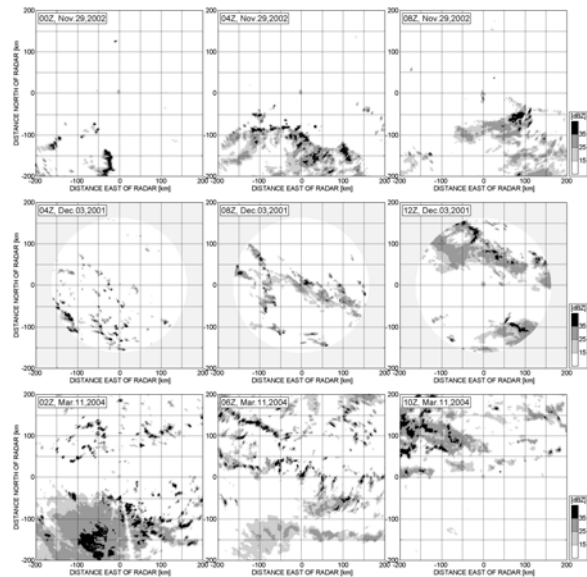


Fig.3: Examples of the 4-hourly radar echo images for type (2) (upper row), (3) (middle row) and (4) (bottom row). The area is 400km x 400km with centered R/V Mirai.

The environmental wind is also different for each types of MCSs. Figure 4 shows that the moving / propagating directions are affected by the low-level (800 hPa) wind in type (2), while upper-level (300 hPa) wind in types (3) and (4). In addition as in Fig. 5, type (2) tends to be organized perpendicular to the low-level wind shear, as in LeMone et al. (1998), while types (3) and (4) do not related to the vertical shear. The internal structure, only obtained for types (3) and (4), shows difference in vertical profile of divergence. The results indicate that the type (2) has the mechanism like the squall-line-type MCS, while type

(4) is the resultant precipitation of propagation of wave. The hybrid type is type (3). With the fact that type (2) appeared principally in the convectively inactive period while type (4) appeared only in the convectively active phase of MJO, the dynamic, thermodynamic and humidity profile could control the appearance of the diurnal MCSs.

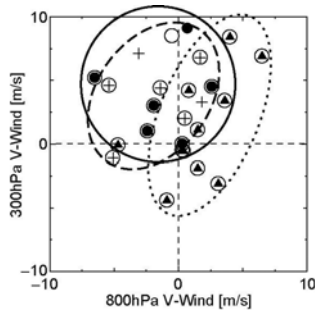


Fig. 4: Relationship between meridional wind (800 hPa at abscissa and 300 hPa at ordinate) and type of MCSs. The triangles, crosses, and filled circles represent MCS of type (2), (3) and (4), respectively. The dotted, break and solid lines indicate the range of distribution for MCS of type (2), (3) and (4), respectively.

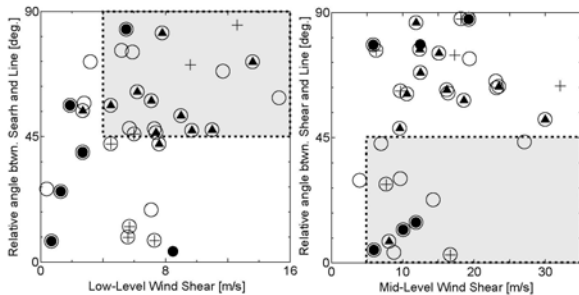


Fig. 5: Relationship between wind shear direction (abscissa) and relative angle between line orientation of MCSs and wind shear direction (ordinate). The left panel is for low-level shear (between 1000 hPa and 800 hPa) and the right panel is for mid-level shear (between 800 hPa and 400 hPa). The marks are same as Fig. 4. The shaded rectangles represent the effective area for shear-normal (left, low-level shear) and shear-parallel (right, mid-level shear) systems, as in LeMone et al. (1998).

6. ATMOSPHERIC DIURNAL RESPONSE

The impacts of these diurnal MCSs to the ambient atmosphere are also examined. The composite analyses of the radiosonde-observed meridional wind (Fig. 6) show the significant anomaly around 12 to 15LT, when the afternoon diurnal MCS appeared. The anomaly is northerly (toward the MCS) in the layer around melting level, and southerly (away from the MCS) below and above. This relationship between MCS and ambient atmosphere is similar to the result of the numerical simulation on the gravity

wave response around MCS (e.g. Nicholls, 1991). On the other hand, the diurnal anomaly of humidity (and mixing ratio of water vapor) shows that the appearance of positive anomaly in middle and upper layer (3 to 8 km) was earlier in the MJO convectively active phase than in than inactive phase, in the afternoon when the diurnal MCSs appeared.

These diurnal anomalies indicate that the diurnal MCSs modify not only in the area where MCSs passed over, but also in the environmental area. The existence of diurnal wave propagation from New Guinea Island, or from convections over New Guinea Island is also suggested.

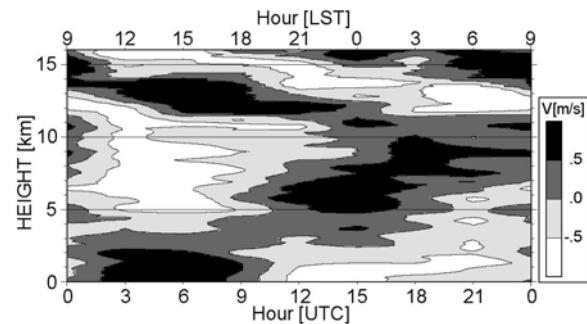


Fig. 6: Averaged diurnal anomaly of meridional wind, obtained by 3-hourly radiosonde observation.

7. SUMMARY AND CONCLUSION

The details of the diurnally appearing propagating precipitating systems were examined by using in-situ observational data at (2N, 138E) for four boreal winters. The radar observation reveals that the diurnal cycle of the precipitation has its peak at local afternoon, and the peak is produced by the appearance of propagating MCSs from the south. The MCSs are categorized as four types. The combined analyses of radiosonde and radar data reveal that the type of MCSs is related to the environmental wind direction and wind shear. The diurnal impact of the diurnal MCS to the environmental wind is also revealed. These results suggest that the diurnal MCSs to the north of New Guinea Island have the mechanism of squall-line type self propagation and wave-like propagation.

[REFERENCES]

- Chen, S. S., and R. A. Houze, Jr., 1997: Diurnal variation and life-cycle of deep convective systems over the tropical Pacific warm pool. *Q. J. R. Meteor. Soc.*, **123**, 357-388.
- Houze, R. A., Jr., S. G. Geotis, F. D. Marks, and A. K. West, 1981: Winter monsoon convection in the vicinity of north Borneo. Part I: Structure and time variation of the clouds and precipitation. *Mon. Wea. Rev.*, **109**, 1595-1614.

- Katsumata, M., K. Yoneyama, Y. Yuuki, S. Sueyoshi, N. Nagahama, and K. Yoshida, 2005: Noise filtering for dual-PRF observed data from R/V Mirai shipborne Doppler radar. *JAMSTEC Rep. Res. Dev.*, **2**, 29-34.
- LeMone, M. A., E. J. Zipser, and S. B. Trier, 1998: The role of environmental shear and thermodynamic conditions in determining the structure and evolution of mesoscale convective systems during TOGA COARE. *J. Atmos. Sci.*, **55**, 3493-3518.
- Liberti, G. L., F. Cheruy and M. Desbois, 2001: Land effect on the diurnal cycle of clouds over the TOGA COARE area, as observed from GMS IR data. *Mon. Wea. Rev.*, **129**, 1500-1517.
- Lukas, R., and E. Lindstrom, 1991: The mixed layer of the western equatorial Pacific ocean. *J. Geophys. Res.*, **96**, 3343-3357.
- Mapes, B.E., T. T. Warner, M. Xu, and A.J. Negri, 2003: Diurnal patterns of rainfall in northwestern South America. Part I: Observations and context. *Mon. Wea. Rev.*, **131**, 799-812.
- Mori, S., Hamada J.-I., Y. I. Tauhid, M. D. Yamanaka, N. Okamoto, F. Murata, N. Sakurai, H. Hashiguchi, and T. Sribimawati, 2004: Diurnal land-sea rainfall peak migration over Sumatera Island, Indonesian maritime continent observed by TRMM satellite and intensive rawinsonde soundings. *Mon. Wea. Rev.*, **132**, 2021-2039.
- Nitta, Ts., and S. Sekine, 1994: Diurnal variation of convective activity over the tropical western Pacific. *J. Meteor. Soc. Japan*, **72**, 627-641.
- Yang, G.-Y., and J. Slingo, 2001: The diurnal cycle in the tropics. *Mon. Wea. Rev.*, **129**, 784-801.
- Yoneyama, K., M. Hanyu, S. Sueyoshi, F. Yoshiura and M. Katsumata, 2002: Radiosonde observation from the ship in the tropical region. *JAMSTECR*, **45**, 31-39.